# Volumetric Multi-Pulse Particle Tracking Measurement for Separated Laminar Transitional Flow Investigations

R. Geisler*, M. Novara and A. Schröder
Institute of Aerodynamics and Flow Technology,
German Aerospace Center (DLR), Göttingen, Germany
* Correspondent author: Reinhard.Geisler@dlr.de

Keywords: STB, particle tracking, micro PTV, laminar flow, transition

ABSTRACT

The new spatiotemporal particle tracking method 'Shake-The-Box' (STB) has been extended to fast burst imaging of four time instants. A corresponding camera system for high resolved volumetric measurements with magnification 1:1 has been developed and adapted to fit within a laminar wing model. The performed measurements cover a volume of 16 mm * 12 mm * 2 mm in close contact to the model surface downstream of a forward facing step. As a result, the boundary layer flow within this volume has been measured with high spatial and temporal resolution for different model configurations.

## 1. Introduction

Particle image velocimetry (PIV, Willert & Gharib 1991) based on the acquisition of two consecutive particle images is nowadays a well-established standard tool for flow investigations. Stereo-PIV provides the instantaneous three-component velocity vector field within a plane and with the development of tomographic PIV (Tomo-PIV, Elsinga et al. 2006) this was extended to the three-component velocity vector field within a three-dimensional volume. However, the gained information about the flow is the spatial distribution of the velocity vectors on an Eulerian grid with only limited and filtered access to further properties (e.g. the instantaneous accelerations). Moreover, the spatial resolution is strictly limited due to the averaging process inherent to the evaluation based on interrogation windows (e.g. by cross-correlation). This applies in particular to tomographic PIV where typical interrogation window sizes are larger than in the stereoscopic approach.

New spatiotemporal concepts such as the 'Shake-The-Box' (STB, Schanz et al. 2013, 2016) particle tracking can overcome these problems and provide complete Lagrangian particle tracks with high spatial resolution, provided a sufficient number of well time-resolved particle images can be captured from a few projections. In applications involving high speed flows or small

interrogation volumes this is often not possible due to the temporal limitations of current high-speed cameras and the power limitations of high-speed illumination lasers. Here, multi-pulse systems based on an extended number of standard (double shutter) PIV cameras and low repetition rate lasers can be an alternative to access high-quality information on the flow. Evaluation of the acquired image data can be based on stereoscopic (Hain & Kähler 2007; Sciacchitano et al. 2012) or tomographic (Lynch & Scarano 2013; Schröder et al. 2013) PIV. However, more accurate results can be achieved with particle tracking approaches; the iterative approach for STB proposed by Novara et al. 2015 can be applied to multi-pulse three-dimensional PIV images in order to reconstruct a large number of short single-particle tracks, therefore offering unprecedented spatial resolution.

## 2. Experimental Setup


**Fig. 1** Laminar wing model in Braunschweig low speed wind tunnel (NWB).

Pressure side with service opening to access the imaging system (left) and suction side with laser light sheet (right) and observation volume on model surface right behind a forward facing step (right, magnified inset).

In the present study, a four-pulse measurement system is used to investigate a forward facing step flow on a laminar flow wing model of 2.7 m chord and 2.2 m span (Fig. 1). The measurements have been performed in the Braunschweig low-speed wind tunnel (NWB) of DNW (German-Dutch Wind Tunnels) with different step heights at low angles of attack and an incoming flow velocity of $U_0$ = 80 m/s. The measurement area is a volume of 16 mm in chord wise (*X*-), 12 mm in span wise (*Y*-) and 2 mm in wall normal (*Z*-) direction, located directly on the model surface immediately downstream of the step in flow direction (Fig. 1, right, magnified inset).

Illumination is provided by two double-cavity InnoLas SpitLight 1000 lasers operating in perpendicular linear polarization states and combined onto the same optical axis by a thin film polarizer. As a result, four illumination pulses can be used to form the light sheet. The four pulses follow each other with alternating polarization states, a short temporal separation (1 µs or 1.5 µs) and a burst repetition rate of 15 Hz. A light sheet of about 2 mm * 20 mm is formed by telescope lenses and diverted by mirrors span wise and glancing onto the model surface (Fig. 1, right). A mirror on the opposite side of the wing reflects back the beam to achieve symmetric scattering properties. Finally, the back-propagating laser light is diverted into a beam dump.

DEHS (Diethylhexyl Sebacate) droplets generated by a set of Laskin-nozzles are used as seeding particles. They are locally injected in the settling chamber of the wind tunnel onto the flow line targeting the measurement volume.

In the measurement area the model surface is formed by a glass window of 1.1 mm thickness (Fig. 1, right, magnified inset). This allows an optical access from within the model for the camera system mounted inside the wing. Four Schneider Macro-Varon 4.5/85 lenses are used to realize a 1:1 magnification of the object volume. The four lines of vision form an in-plane geometry with an angular offset of 20° each (Fig. 3). A mirror diverts the object plane through the glass window onto the model surface and thus implements a field of view in close contact to the model surface and immediately downstream the surface step (Fig. 2).

Two PCO.edge cameras are placed in the image planes of the central lenses. These lenses are equipped with linear polarization filters, one adjusted to block the light from the first laser and the other to block the light from the second one. Behind each of the outer lenses a thin film polarizer separates the light with the two polarization states to different optical axes and thus enables to capture the images illuminated by each of the two lasers with a different PCO.edge camera, respectively (Fig. 3). In summary, the camera setup depicted in Fig. 4 forms a system of three cameras for each of the two polarization states. It can capture images from a volume of

16 mm * 12 mm * 2 mm in close contact to the model surface with magnification of 1:1 corresponding to a pixel resolution of about 6.5 µm.

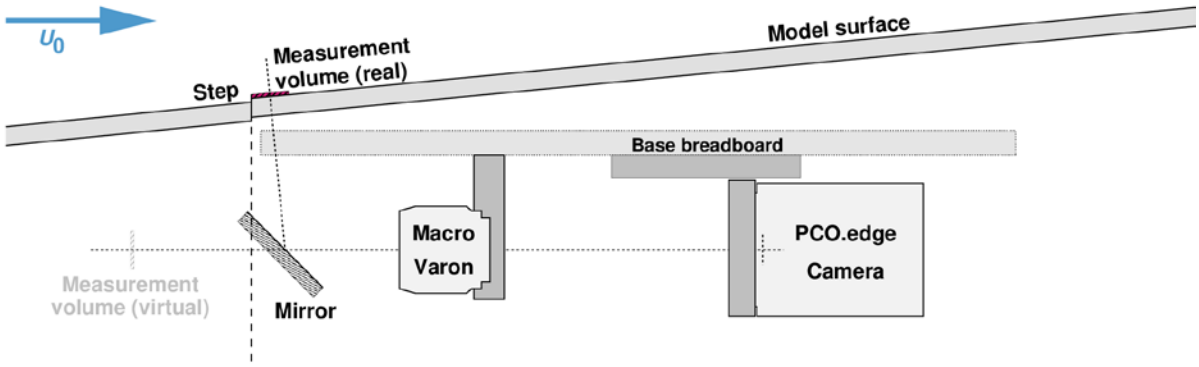


**Fig. 2** Sketch of the camera setup, side view. Through a glass plate in the model surface, a 1:1 image of the measurement volume is captured by cameras inside the model

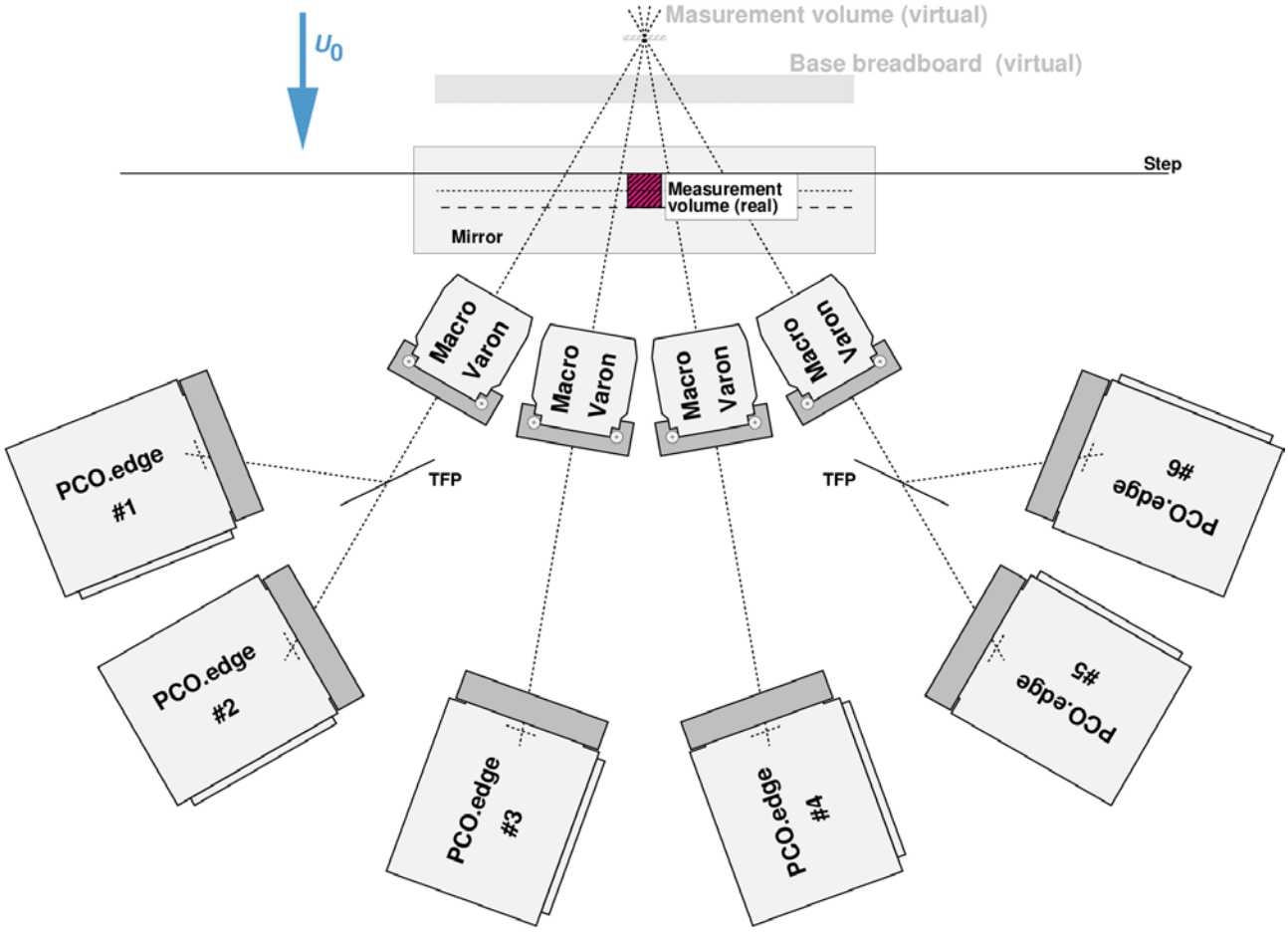


**Fig. 3** Sketch of the camera setup, top view. Thin film polarizers (TFP) enable the outer two camera pairs to capture different polarization states, respectively. The two central cameras in turn capture different polarization states by means of adjusted polarization filters.

**Fig. 4** Camera system mounted inside the wing model.

## 3. Results

Several measurements have been performed with different step heights and low angles of attack close to a lift of zero at a free flow velocity of $U_0$ = 80 m/s. The acquired images are processed by means of the iterative STB tracking algorithm optimized for the low numbers of samples within one imaging burst typical of multi-pulse investigations. For a detailed description of the processing strategy and parameters the authors refer to Novara et al. 2015.

First results show that each imaging burst finally gives a volumetric snapshot of about 5000 particles tracked over four positions (Fig. 5) with a positional accuracy of about 0.1 pixel (derived from the analysis of synthetic images, Schanz et al. 2016). The relatively low particle number per snapshot is due to the high image magnification and the seeding density limitations given for the anechoic test section of the NWB.

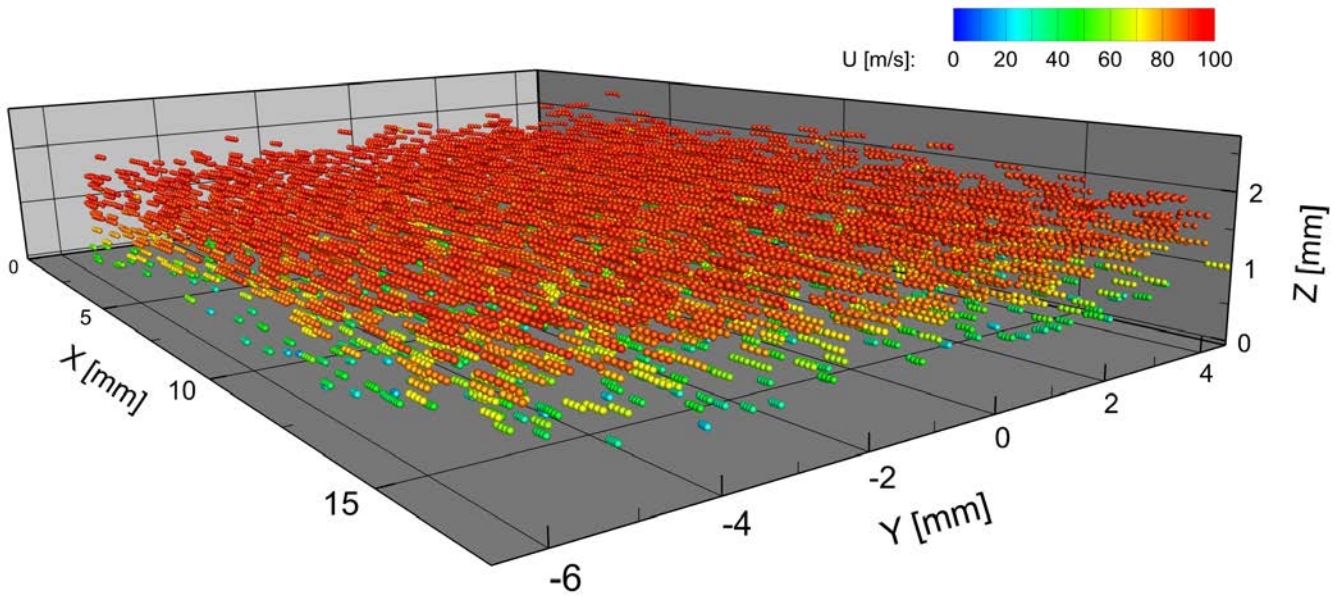


**Fig. 5** Snapshot with reconstructed tracks of ~5000 particles, color-coded by stream wise velocity component.

Step height 0.85 mm at position at $X$ = 0 mm, flow in positive $X$-direction, angle of attack $\alpha$ = 1°.

The particle position along the track is fitted by means of a second order polynomial; the velocity is evaluated analytically from the fit at the mid-point location of the single tracks. Since the flow is independent of the span wise $Y$-position (2D profile), an ensemble averaging process can be applied to evaluate the flow statistics where two-dimensional bins in X- and Z- directions are used to collect the velocity samples over the complete span-wise Y- direction. Given the chosen bin size of 270 µm and 27 µm (along X- and Z- respectively) at least 400 independent samples are available per bin for the evaluation of the mean velocity profile shown in Fig. 6, 7.

Depending on the flow configuration, in the lowermost volume very few or even no particles have been detected (Fig. 7). Here, due to the aerodynamic surface load, the model is slightly deformed to a concave shape and thus the particle illumination is shaded.

As for any particle tracking approach, results are obtained at scattered locations within the investigated volume corresponding to the particle locations (Fig. 5); an interpolation method based on cubic B-splines and penalizing divergence of velocity (FlowFit, Gesemann 2015) is used to transform the velocity results from the arbitrary distribution of particle tracks to a regular grid. The velocity fluctuation field is calculated by subtracting the average velocity vector field from each of the instantaneous velocity fields. Here again, in addition to the temporal averaging a spatial one in span wise direction is applied to reach statistical significance. In Fig. 8 to 10, a selected plane of the instantaneous velocity fluctuation fields (typical samples) together with the corresponding RMS value profile is depicted for different configurations.

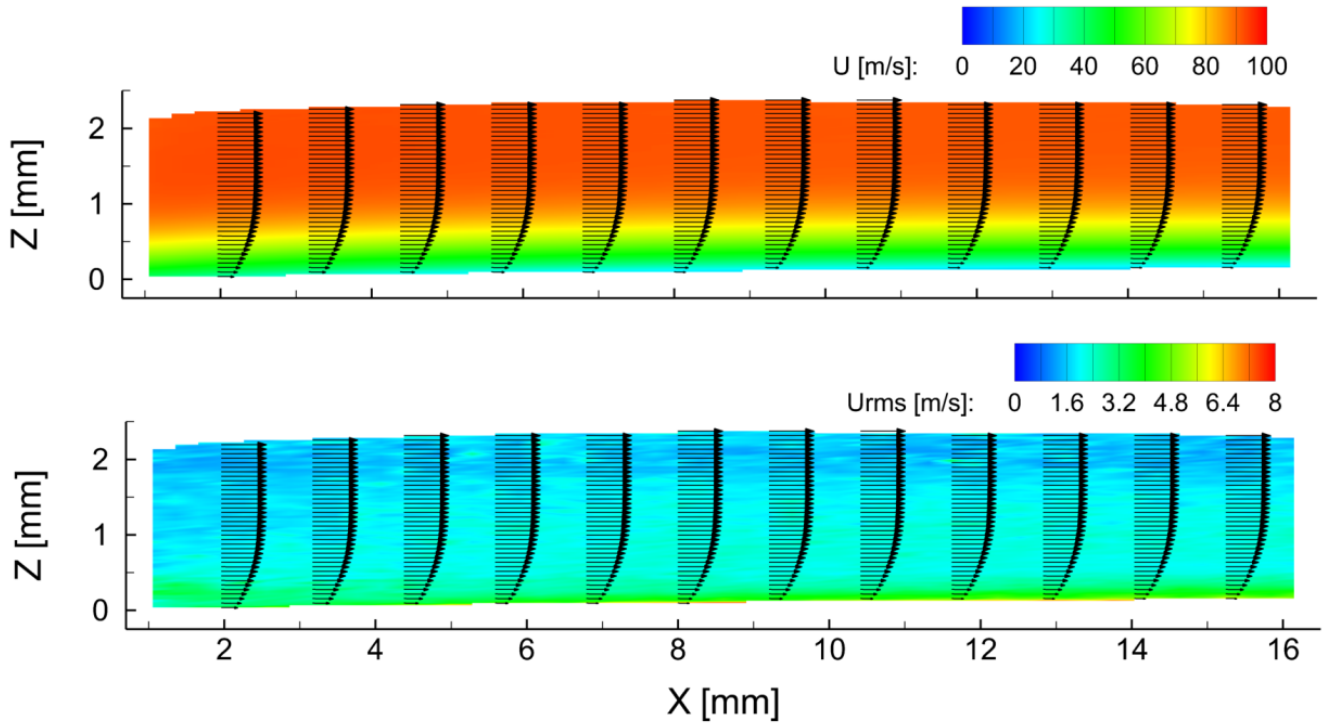


**Fig. 6** Averaged velocity profile (top) and RMS values (bottom) for step height 0.85 mm and angle of attack α = 1°.

Average over 10000 recordings with ~5000 particle tracks each.

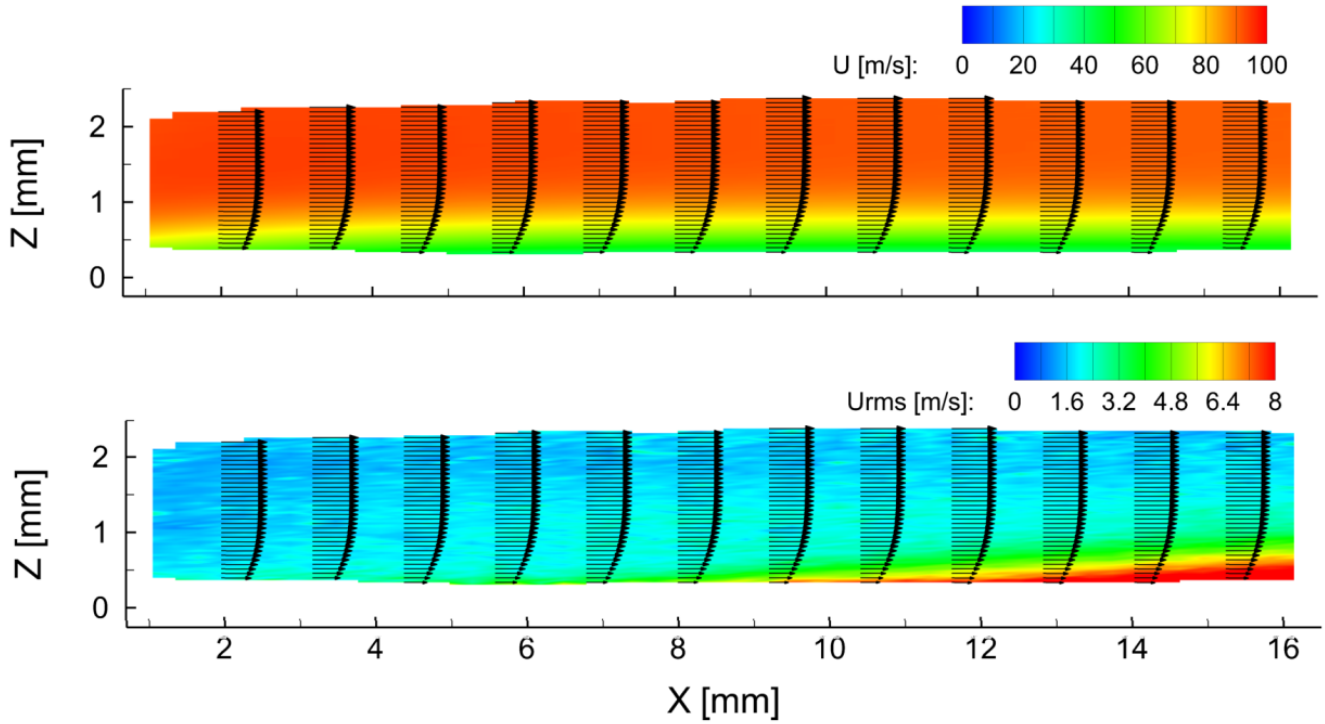


**Fig. 7** Averaged velocity profile (top) and RMS values (bottom) for step height 1.05 mm and angle of attack α = -0.3°.

Average over 8800 recordings with ~5000 particle tracks each.

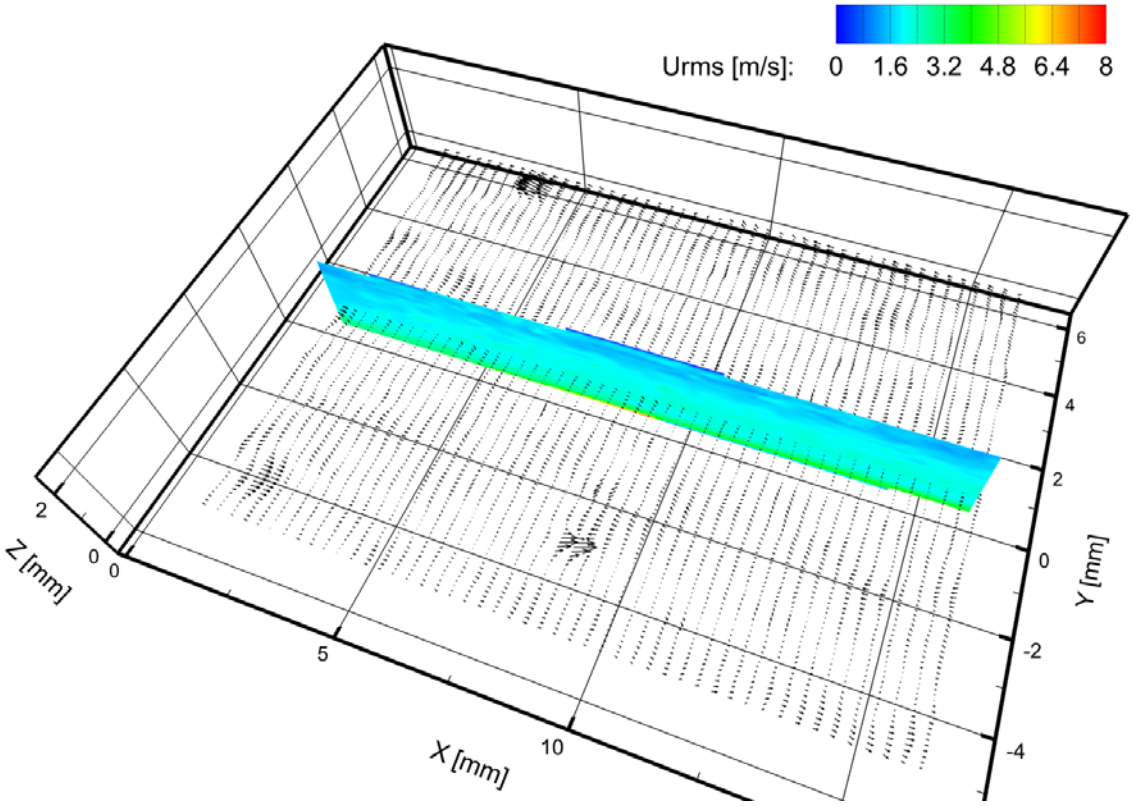


**Fig. 8** Instantaneous velocity fluctuations (typical sample) and RMS for step height 0.85 mm and angle of attack $\alpha$ = 1°.

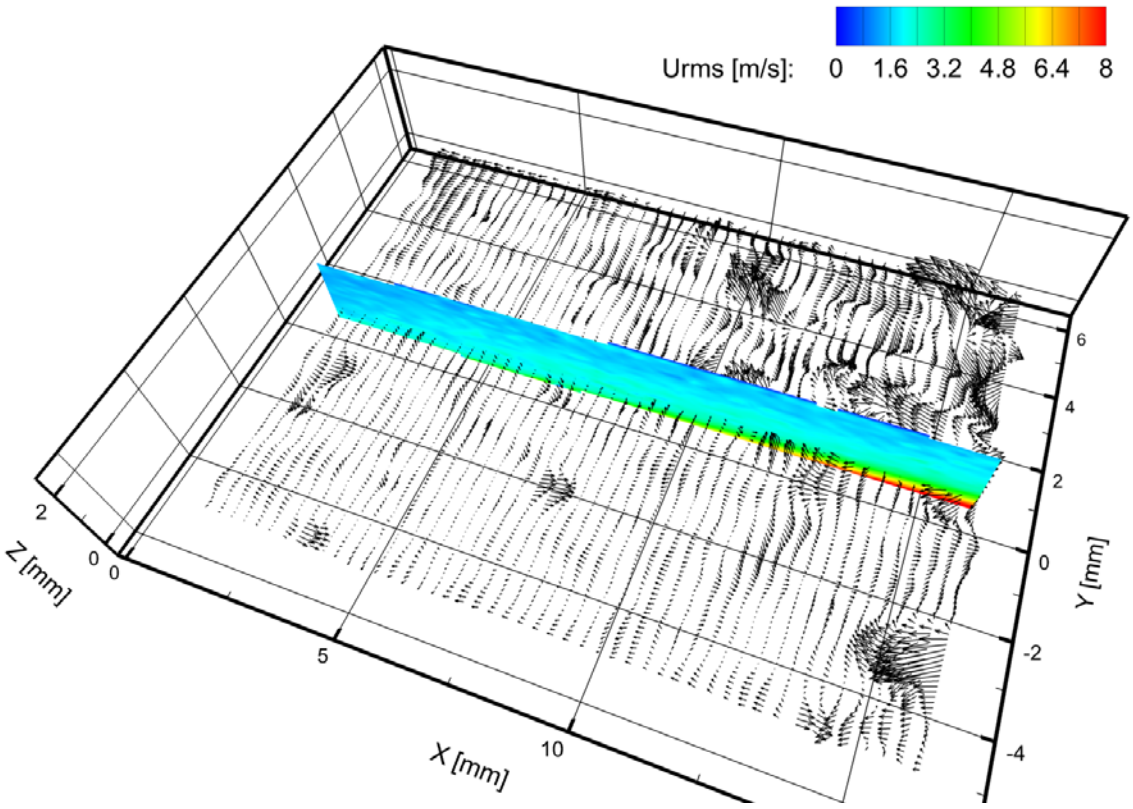


**Fig. 9** Instantaneous velocity fluctuations (typical sample) and RMS for step height 1.05 mm and angle of attack $\alpha$ = -0.3°.

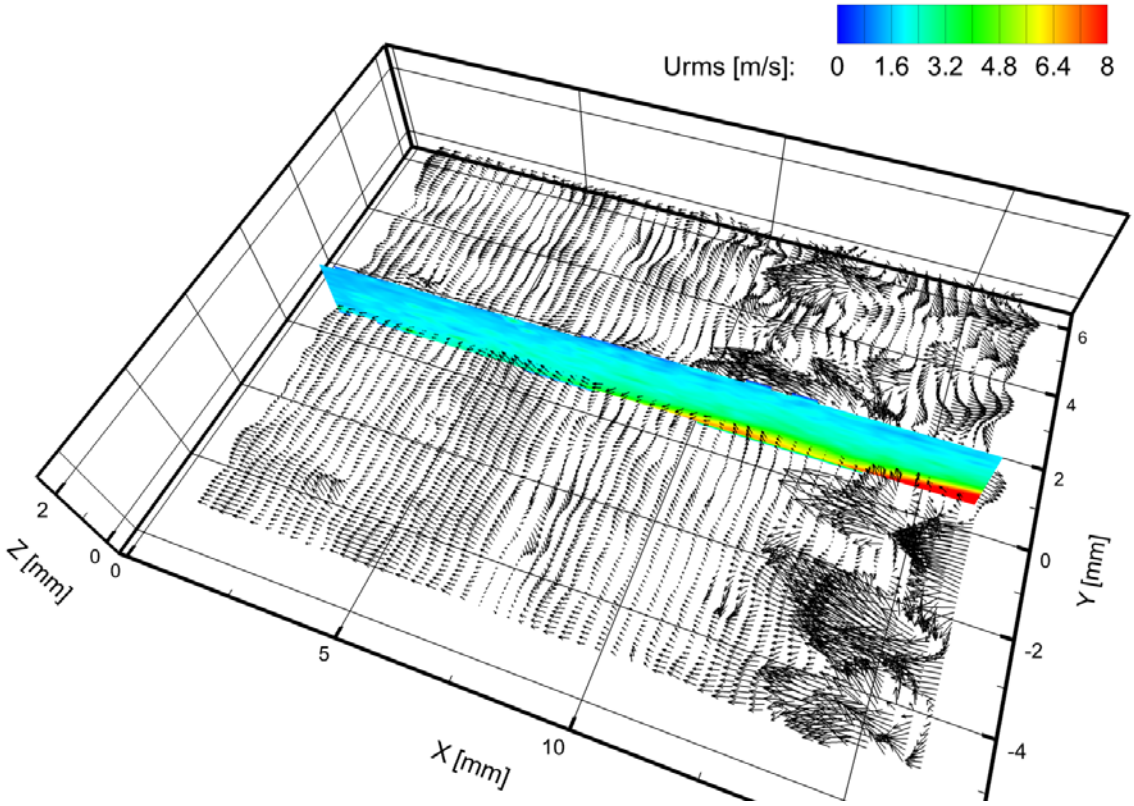


**Fig. 10** Instantaneous velocity fluctuations (typical sample) and RMS for step height 1.05 mm and angle of attack α = -0.3°, with acoustic excitation.

The larger fluctuations observed in Fig. 9, with respect to Fig. 8, occur as a consequence of the larger step height and suggest the presence of fast growing transitional boundary- and shear layer instabilities above a flat near-wall laminar separation bubble. The flow structures visible in the instantaneous velocity fluctuations in Fig. 9 and 10 are s.c. 'spikes ' arising usually at the tip of lambda- vortices as a consequence of a non-linear development of the initial linear TS- or KH-wave instabilities, similar to K-type transition. Those spikes are penetrating through the measurement volume (see extracted plane) and are more or less arranged in spanwise rows for the given phase locked multi-pulse STB measurements with respect to the acoustic wave excitation. The increased intensity of the corresponding fluctuations with acoustic excitation are caused by an appropriate choice of the acoustic disturbance frequency and amplitude, leading to high receptivity with respect to the linear stability diagram of the given transitional scenario and further on to large grow rates of the disturbance waves, Fig. 10.

The present study was part of the project ATLATUS (Aero-Testing on LAminar wings with disTUrbanceS) within the LUFO IV compound project ProWinGS (PeRfOrmance development for WINg design, Ground tests and Simulations).

**References**


- Elsinga GE, Scarano F, Wieneke B, van Oudheusden BW (2006) Tomographic particle image velocimetry, Exp Fluids 41: 933-947
- Gesemann S (2015) From Particle Tracks to Velocity and Acceleration Fields Using B-Splines and Penalties. arXiv:1510.09034
- Hain R, Kähler CJ (2007) Fundamentals of multiframe particle image velocimetry (PIV). Exp Fluids 42: 575–587
- Lynch K, Scarano F (2013) Material Derivative Measurements in High-Speed Flows by Four-Pulse Tomographic PIV. 10th International Symposium on Particle Image Velocimetry, Delft, The Netherlands
- Novara M, Schanz D, Kähler C J, Schröder A (2015) Shake-The-Box for multi-pulse tomographic systems: towards high seeding density particle tracking in high speed flows, 11th International Symposium on Particle Image Velocimetry, Santa Barbara, CA USA
- Schanz D, Gesemann S and Schröder A "Shake-The-Box: Lagrangian particle tracking at high particle image densities" Exp In Fluids (2016, accepted for publication)
- Schanz D, Schröder A, Gesemann S, Michaelis D, Wieneke B (2013) "Shake-the-Box: a highly efficient and accurate Tomographic Particle Tracking Velocimetry (TOMO-PTV) method using prediction of particle position" 10th International Symposium on Particle Image Velocimetry, Delft, The Netherlands
- Schröder A, Schanz D, Geisler R, Willert C, Michaelis D (2013) Dual-Volume and Four-Pulse Tomo PIV using polarized laser light. 10th International Symposium on Particle Image Velocimetry, Delft, The Netherlands
- Sciacchitano A, Scarano F, Wieneke B (2012) Multi-frame pyramid correlation for time-resolved PIV. Exp Fluids 53: 1087–1105
- Willert CE, Gharib M (1991) Digital particle image velocimetry. Exp Fluids 10: 181–193